

Accepted manuscript (author version)

To appear in: **Majlesi Journal of Electrical Engineering (MJEE)**

Online ISSN: 2345-377X

Print ISSN: 2345-3796

This PDF file is not the final version of the record. This version will undergo further copyediting, typesetting, and production review before being published in its definitive form. We are sharing this version to provide early access to the article. Please be aware that errors that could impact the content may be identified during the production process, and all legal disclaimers applicable to the journal remain valid.

Received: 30-Jul-2025

Revised: 06-Sep-2025

Accepted: 20-Dec-2025




This article has license CC BY 4.0 <https://creativecommons.org/licenses/by/4.0/>

Original Research

Interpretable Epileptic Seizure Detection Using Entropy and Gram Matrix Features in Beta–Gamma Bands

Shiva Rasaei Salari¹, Hamed Erfankhah¹

1- Department of Electrical and Biomedical Engineering, Ur.C., Islamic Azad University, Urmia, Iran.
Emails: rasaishiva4@gmail.com, erfankhah_hamed@iau.ac.ir (Corresponding author) 

© Author(s) 2025

Abstract

Epileptic seizure detection using EEG is vital for clinical diagnosis. This paper proposes a novel, interpretable framework for automated seizure classification based on entropy features from Beta (12–30 Hz) and Gamma (30–60 Hz) bands. The Discrete Legendre Transform (DLT) decomposes EEG signals, enabling extraction of four entropy measures: Approximate, Permutation, Sample, and Fuzzy Entropy. To capture inter-feature dependencies, Gram Matrix modeling is applied, yielding four global descriptors (trace, Frobenius norm, max eigenvalue, determinant), fused into a 12-dimensional feature vector. Evaluated with SVM and ProCRC classifiers on two datasets, Bonn (interictal D vs. ictal E) and independent Hauz Khas (HK, interictal vs. ictal), the method achieves **100% accuracy on Bonn** and **97.5% on HK** under 60–40 stratified split, and **99.5% (Bonn)** and **97% (HK)** under 10-fold cross-validation. Performance surpasses multiple state-of-the-art methods, including deep and hybrid models, while remaining fully interpretable, lightweight, and free of deep learning, image conversion, or GPU dependency. The framework's transparency, computational frugality, and cross-dataset robustness make it highly suitable for portable, real-world clinical deployment in resource-limited settings. This work confirms that high diagnostic accuracy and interpretability are not mutually exclusive in seizure detection.

Keywords: Epileptic seizure detection, Electroencephalographic signal analysis, Gamma and Beta band entropy, Gram matrix modeling, Probabilistic collaborative representation.

1. INTRODUCTION

Electroencephalogram (EEG) signals have become a cornerstone in non-invasive brain monitoring, with diverse applications in clinical and cognitive neuroscience. Recent studies have demonstrated their utility in automatic detection of sleep spindles using hybrid ANN-SVM classifiers [1], as well as in sleep stage classification by applying Laplacian scoring for feature selection from single-channel data [2], analysis of neural pattern alterations in substance use disorders [3], and development of non-invasive brain-computer interfaces (BCIs) for decoding motor intentions such as left/right hand movement [4]. These works highlight the versatility of EEG in capturing subtle neurological dynamics across various pathological and physiological states. Despite differing objectives, they share common challenges—including signal non-stationarity, noise sensitivity, and the need for robust, interpretable feature extraction and classification methods—challenges that are also central to epileptic seizure detection.

With more than 50 million cases worldwide, epilepsy ranks among the most common neurological disorders, as reported by the World Health Organization (WHO) [5]. The core mechanism of epileptic seizures involves abnormal, self-sustaining electrical discharges in the brain, which disrupt normal cortical function and can be captured via EEG for automated detection. In clinical neurophysiology, EEG is widely employed for epilepsy diagnosis, leveraging its capacity to detect transient pathological discharges with high temporal accuracy and minimal patient burden. [6]. As EEG datasets grow in duration and complexity, manual review becomes impractical, motivating the need for automated, objective, and reproducible analysis tools in epilepsy care.



Therefore, developing accurate, efficient, and interpretable automated seizure detection systems is crucial for improving patient care and reducing the diagnostic burden.

The transient and nonlinear nature of epileptic discharges introduces significant morphological diversity in EEG, challenging conventional classifiers and motivating the use of dynamic and interpretable models [7]. These characteristics—non-stationarity, nonlinearity, and high complexity—challenge traditional signal processing methods and necessitate advanced feature extraction and classification techniques.

Over time, seizure detection strategies have advanced from time-frequency analysis of raw EEG to mapping signals into visual domains (e.g., spectrograms, Gramian matrices) and leveraging deep architectures for automated feature discovery.

Signal-based methods extract features directly from raw or transformed EEG signals. Baghaie et al. [8] utilized wavelet transform and chaos theory to extract features from EEG sub-bands, employing measures such as correlation dimension and Lyapunov exponent to characterize nonlinear dynamics. Fuzzy subtractive clustering and ensemble averaging achieved classification accuracies of 96.8% and 97.5%, respectively, outperforming visual inspection by neurologists, which typically does not exceed 80%. Kannathal et al. [9] demonstrated the effectiveness of entropy and nonlinear dynamics in distinguishing normal from ictal EEG patterns. To address computational constraints in wearable systems, lightweight entropy-based frameworks have been proposed, such as the bitwise entropy estimation method in [10], which achieved 97.13% average accuracy across multiple binary tasks. Dimensionality reduction techniques like PCA and ICA, along with feature selection methods such as Genetic Algorithms [11], have further enhanced performance by eliminating redundancy.

Image-based approaches transform EEG signals into time-frequency representations (e.g., via STFT) and apply computer vision techniques. In [12], time-frequency maps were treated as images, and textural features (GLCM, LBP, TFCM) were extracted to quantify local patterns, which were then passed to an SVM classifier for seizure detection. Similarly, [13] applied Histogram of Oriented Gradients (HOG) to STFT-based images, achieving 98.0% accuracy. Other studies, such as [14], used 2D Discrete Wavelet Transform (DWT) on time-frequency maps for spatial feature extraction, again combined with SVM classifiers.

Recently, deep learning techniques have emerged as dominant in seizure detection, leveraging their capacity to automatically discover multi-level features from raw or transformed EEG inputs without reliance on handcrafted descriptors. In [15], deep autoencoders were trained on 2D/3D spectrograms for end-to-end classification. Zeng et al. [16] proposed a hybrid model combining CNN-based feature learning with Principal Component Analysis (PCA) and shallow classifiers. Xin et al. [17] introduced an attention-based Wavelet-CNN that integrates multi-scale wavelet decomposition with convolutional layers and attention mechanisms, achieving 99.11% accuracy on the Bonn dataset. While these models show high performance, they often require large labeled datasets, extensive computational resources, and suffer from limited interpretability—hindering clinical trust and deployment in resource-constrained environments.

The selection of the Beta (12–30 Hz) and Gamma (30–60 Hz) bands is supported by neurophysiological evidence showing that high-frequency oscillations (HFOs) in these ranges increase during epileptic activity and reflect abnormal cortical synchronization in the epileptogenic zone [18]. Although ictal EEG often contains strong low-frequency components, several studies have demonstrated that Beta and Gamma rhythms exhibit marked changes, such as increased power, reduced entropy, and localized hypersynchrony, during ictal episodes compared with interictal background activity. These alterations capture fast-scale neuronal dynamics that are not represented in the lower-frequency delta–theta rhythms and therefore provide discriminative biomarkers for distinguishing interictal from ictal states in the Bonn dataset.

This work introduces a compact and fully interpretable model for detecting epileptic seizures from single-channel EEG. We extract entropy features (ApEn, SampEn, PermEn, FuzzyEn) from Beta and Gamma bands—frequencies associated with cortical activation during seizures—using Discrete Legendre Transform (DLT) for spectral decomposition. A Gram Matrix is then constructed to model second-order feature correlations, and global descriptors (trace, Frobenius norm, maximum eigenvalue, determinant) are fused with entropy features. The enriched feature vector is classified using SVM with RBF kernel and Probabilistic Collaborative Representation-Based Classifier (ProCRC). Evaluated on two publicly available EEG datasets, the Bonn University dataset (Groups D and E) and the independent Hauz Khas (HK) clinical dataset (interictal vs. ictal), our method achieves up to 100% accuracy on Bonn and 97.5% on HK under stratified train/test split, outperforming many existing approaches. Importantly, the proposed framework avoids deep learning, offers full transparency, and is suitable for portable and wearable diagnostic devices.

This work makes the following contributions:

- 1- A hybrid feature extraction framework combining entropy analysis in Beta and Gamma frequency bands with Gram Matrix modeling to enhance feature representation through second-order statistics.



- 2- Introduction of global Gram Matrix descriptors (trace, Frobenius norm, maximum eigenvalue, determinant) as complementary features to capture inter-feature correlations and improve discriminative power.
- 3- Integration of the Probabilistic Collaborative Representation-Based Classifier (ProCRC) into EEG-based seizure detection, offering enhanced generalization and probabilistic interpretation.
- 4- Experimental validation across two independent EEG benchmarks, confirming robust performance without dataset-specific tuning: 100% accuracy on the canonical Bonn D–E task and 97.5% on the clinically derived Hauz Khas interictal–ictal task, all achieved with a fully interpretable, non-deep pipeline.
- 5- Design of a lightweight, interpretable pipeline suitable for embedded implementation in resource-limited settings.

The remainder of this paper is organized as follows. Section 2 describes the dataset and details the proposed framework, including signal preprocessing, entropy-based feature extraction, Gram matrix modeling, and classification. Section 3 presents the experimental results and comparative analyses with state-of-the-art methods on both the Bonn and Hauz Khas datasets. Section 4 provides an in-depth discussion of the results, highlighting their physiological and methodological implications. Section 5 outlines the limitations of the present study. Section 6 discusses potential directions for future research, and finally, Section 7 concludes the paper by summarizing the main contributions.

2. MATERIALS AND METHODS

2.1. Database

The experiments are conducted using two publicly available EEG datasets to ensure both benchmarking and generalizability assessment.

Bonn University EEG Dataset — The primary dataset is the well-established Bonn University EEG database [19], widely used in epilepsy research. This dataset consists of EEG recordings collected from both healthy subjects and epileptic patients under controlled conditions. The signals were recorded using a standardized protocol with a sampling rate of 173.61 Hz, and each file contains exactly 4097 data points, corresponding to approximately 23.6 seconds of recording. The dataset includes five distinct categories of EEG recordings, denoted by the letters Z, O, N, F, and S, representing different physiological and pathological states:

- A: Z (Surface EEG recordings from healthy subjects with eyes open)
- B: O (Resting-state EEG from healthy individuals with eyes closed, reflecting normal background activity)
- C: N (Interictal (non-seizure) intracranial EEG activity recorded from within the seizure-free zone of epileptic patients)
- D: F (Interictal EEG activity recorded from the epileptogenic zone of epileptic patients)
- E: S (Ictal (seizure) EEG segments recorded during seizure activity)

Each EEG recording was obtained using the same acquisition equipment and preprocessing settings, ensuring consistency across all samples. The signals were bandpass filtered between 0.5 Hz and 85 Hz, and digitized at a resolution of 12 bits per sample. In this study, we focus on the binary classification task between Group D (interictal) and Group E (ictal), which is a commonly adopted scenario in seizure detection research. This comparison aims to distinguish between interictal and ictal events. A total of 200 EEG segments were selected for analysis, 100 from Group D and 100 from Group E, to ensure class balance and avoid bias toward any specific brain state. Fig. 1(a) illustrates sample EEG segments from this dataset, highlighting characteristic patterns in interictal and ictal states. As shown in Fig.1(a), seizure EEG segments exhibit higher amplitude fluctuations and more synchronized oscillatory behavior compared to interictal segments.

Hauz Khas (HK) EEG Dataset — To assess cross-dataset robustness, we further evaluate the proposed framework on the Hauz Khas (HK) EEG dataset [20], a publicly available clinical dataset recorded from epileptic patients at the Neurology and Sleep Center, New Delhi. The data were acquired using the international 10–20 electrode system at a sampling rate of 200 Hz, with bandpass filtering (0.5–70 Hz), and subdivided into three clinical phases: preictal, interictal, and ictal, each containing 50 non-overlapping segments (total: 150 segments).

For compatibility with our primary Bonn-based binary task (D vs. E), we selected the interictal and ictal subsets (50 + 50 = 100 segments), ensuring perfect class balance. Fig. 1(b) displays interictal and ictal recordings from the HK dataset.

Fig. 2 illustrates the architecture of the proposed automated seizure detection framework. The method contains the following steps.

2.2. Preprocessing Steps

To prepare the data for feature extraction, the following preprocessing steps were applied:

- 1- **Normalization:** Each EEG segment was standardized to have a mean of zero and a standard deviation



of one in order to eliminate amplitude variations across subjects.

- 2- **Segmentation:** Although each file contains a fixed-length epoch (4097 samples), they were treated as individual instances without further splitting to preserve temporal integrity.
- 3- **Artifact Removal:** Visual examination was conducted to eliminate epochs corrupted by disturbances such as ocular blinks or muscular activity. No additional filtering was applied beyond the standard preprocessing included in the dataset.
- 4- **EEG rhythms decomposition based on discrete Legendre transform (DLT):** The isolation of β and γ oscillations was performed using Jacobi polynomial transform (JPT) [21].

Unlike Fast Fourier Transform (FFT), which assumes stationarity and periodicity of the signal, DLT uses discrete Legendre polynomials to represent EEG segments in an orthonormal basis. This allows for accurate frequency decomposition even in the presence of non-stationary and transient components commonly found in epileptic EEG recordings.

The realization of this approach is outlined as follows [21]:

$$\left\{ \begin{array}{l} \alpha_k = \frac{2k+1}{M(M+1)} \sum_{j=0}^M \frac{L_k(x_j)}{[L_M(x_j)]^2} s(x_j), \quad k=0,1,\dots,M-1 \\ \alpha_M = \frac{1}{M+1} \sum_{j=0}^M \frac{s(x_j)}{L_M(x_j)}, \quad k=M \end{array} \right. \quad (1)$$

Where α_k denotes the projection of signals onto the Jacobi basis element $J_k^{\alpha,\beta}$ and M represents the degree of approximation. To identify the spectral coefficients associated with β and γ oscillations, the Fourier transform is used. The extracted rhythms for each selected spectral coefficients is as follows:

$$s(x) = \sum_{k=0}^M \alpha_k J_k^{\alpha,\beta} \quad (2)$$

Fig. 3 presents sample EEG segments from the Bonn University dataset, along with their corresponding spectral coefficients obtained using the DLT. The top shows a raw EEG signal from Group F (or D), while the bottom column displays seizure EEG activity from Group S(or E), highlighting notable differences in amplitude and oscillatory patterns. Additionally, the extracted β (12–30 Hz) and γ (30–60 Hz) rhythms are shown alongside their Fast amplitude spectrum (AS) to illustrate the dominant components in each band. One key advantage of the DLT is its ability to extract β and γ band components in a single decomposition step. This contrasts with wavelet-based methods such as DWT, which typically require multiple decomposition levels and filter bank stages to isolate specific frequency bands.

2.3. Feature Extraction

The primary objective of feature extraction is to reduce the dimensionality of raw EEG signals while preserving discriminative patterns that distinguish ictal from interictal brain activity. Following frequency band decomposition using the DLT, a comprehensive set of features is extracted, including entropy measures such as Approximate Entropy (ApEn), Permutation Entropy (PermEn), Sample Entropy (SampEn), and Fuzzy Entropy (FuzzyEn). Additionally, statistical features derived from the Gram Matrix are incorporated to model internal correlations among extracted patterns. These features collectively capture key oscillatory characteristics within the β and γ frequency bands, thereby enhancing the system's ability to discriminate between different brain states without relying on high-dimensional input representations.

The choice of these four entropy measures, ApEn, SampEn, PermEn, and FuzzyEn, is motivated by their complementary roles in capturing distinct aspects of EEG dynamics: ApEn and SampEn quantify amplitude-based regularity (with SampEn offering improved bias resistance), PermEn reflects temporal ordering through ordinal pattern analysis (and is robust to noise without amplitude assumptions), and FuzzyEn softens similarity matching via fuzzy logic to reduce sensitivity to artifacts. Together, they provide a richer, multi-faceted characterization of signal complexity while remaining suitable for short, nonstationary, and artifact-prone clinical EEG segments.

2.3.1. Approximate Entropy (ApEn)

Approximate Entropy (ApEn) is a nonlinear metric that assesses the regularity and unpredictability of physiological signals, including EEG [22]. It quantifies the probability that sequences of observations with similar initial patterns continue to match as the signal evolves. A lower ApEn value indicates higher predictability and regularity, often observed during seizure states due to increased neuronal synchronization. Mathematically, Given a time series $x(i), 1 < i < N$, ApEn is computed as:



$$ApEn(m, r, N) = \phi^m(r) - \phi^{m+1}(r) \quad (3)$$

Where m denotes embedding dimension, r represents the similarity threshold, and N is the number of data points in the signal. The term $\phi^m(r)$ corresponds to the average logarithmic likelihood that sequences similar for m points remain similar at the next point.

In epileptic EEG signals, ApEn tends to decrease during seizure (ictal) states due to increased signal regularity and synchronization of neuronal activity. In contrast, higher ApEn values are observed in non-seizure (interictal) states, reflecting greater complexity and unpredictability. The parameter set $m=2$, $r=0.2$ is widely adopted in biomedical research.

2.3.2. Permutation Entropy (PermEn)

Permutation Entropy (PermEn) quantifies signal complexity by analyzing the frequency of ordinal patterns in embedded time series, which provides a robust and computationally efficient way to analyze nonlinear dynamics in EEG signals [23]. It quantifies the irregularity of a signal by evaluating the distribution of permutation patterns derived from its embedding vectors. Given a time series $x(i)$, $1 < i < N$ with embedding dimension m and a time delay τ , all subsequences of length m are converted into one of $m!$ symbolic permutations according to the rank order of their elements. The probability p_i of each permutation pattern is estimated, and PermEn is computed as:

$$PermEn(m, \tau, N) = - \sum_{i=1}^{m!} p_i \ln(p_i) \quad (4)$$

Higher PermEn values indicate greater signal complexity and unpredictability, while lower values reflect regularity and synchronization.

In epileptic EEG analysis, PermEn decreases significantly during seizure (ictal) states due to increased neural synchronization. This makes it a highly effective feature for distinguishing between interictal and ictal brain activity. In biomedical signal analysis, common choices for permutation entropy include an embedding dimension of $m=3$ or 4 and a time delay of $\tau=1$.

2.3.3. Sample Entropy (SampEn)

Sample Entropy (SampEn) is a modification of ApEn that avoids self-matching and provides more consistent results for short and noisy physiological signals such as EEG [24]. It calculates the negative log-probability that two distinct sequences of length m , similar within a tolerance r , will remain similar when extended by one sample.

Mathematically, given a time series $x(i)$, $1 < i < N$, the SampEn is defined as:

$$SampEn(m, r, N) = - \ln \left(\frac{C^{m+1}(r)}{C^m(r)} \right) \quad (5)$$

Where $C^m(r)$ is the number of template matches of length m within tolerance r , and $C^{m+1}(r)$ is the same for length $m+1$. Unlike Approximate Entropy (ApEn), SampEn excludes self-matches, making it less biased and more consistent, especially for short and noisy biomedical signals. In epileptic EEG analysis, SampEn decreases significantly during ictal (seizure) states due to increased signal regularity and neural synchronization. This makes it a highly discriminative feature for automated seizure detection. SampEn is computed with $m=2$ and $r=0.2$, following established guidelines for EEG analysis.

2.3.4. Fuzzy Entropy (FuzzyEn)

Fuzzy Entropy (FuzzyEn) is a nonlinear complexity measure that evaluates the regularity of physiological signals by using fuzzy membership functions instead of Heaviside functions [25]. This approach provides smoother transitions and reduces sensitivity to abrupt changes in template matching, making it particularly suitable for noisy biomedical signals like EEG.

Given a time series $x(i)$, $1 < i < N$, the fuzzy similarity between two vectors of length m is defined using a Gaussian-type membership function:



$$d_{ij}^m = e^{-\left(\frac{D_{ij}^m}{r}\right)^n} \quad (6)$$

Where D_{ij}^m is the distance between vectors i and j , r is the tolerance threshold, and n controls the gradient of the boundary. FuzzyEn is then computed as:

$$\text{FuzzyEn}(m, r, n) = \ln \frac{\phi^m(r)}{\phi^{m+r}(r)} \quad (7)$$

Where $\phi^m(r)$ indicates the average fuzzy similarity of all template matches of length m . Lower FuzzyEn values indicate higher regularity and synchronization, which are characteristic of epileptic seizure (ictal) states. In contrast, higher values reflect complex and unpredictable brain activity during non-seizure (interictal) periods. The parameter set $m=2$, $r=0.2 \times \text{SD}$ and $n=2$ is extensively used in biomedical research.

2.3.5. Gram Matrix Modeling for Feature Enhancement

To capture internal correlations between extracted features and enhance the discriminative power of the representation, we applied Gram Matrix modeling on the feature matrix. The Gram Matrix is a widely used tool in signal processing and machine learning to quantify pairwise similarity among samples [26]. Given a feature vector $F \in R^d$, the Gram Matrix $G \in R^{d \times d}$ is computed as:

$$G = F \cdot F^T \quad (8)$$

This results in a symmetric matrix where each element G_{ij} reflects the correlation between the i -th and j -th features in the vector. By analyzing this matrix, we can extract second-order statistical features that go beyond first order descriptors like mean or variance.

From the Gram Matrix, we derive the following global descriptors:

- **Trace:** $\text{Tr}(G) = \sum_{i=1}^d G_{ii}$ – represents total energy of the feature set.
- **Frobenius Norm:** $\|G\|_F = \sqrt{\sum_{i,j} G_{ij}^2}$ – indicates overall feature variability.
- **Determinant:** $\det(G)$ – reflects the volume of space covered by the feature vectors.
- **Maximum Eigenvalue:** λ_{\max} – highlights dominant direction of variation.

These features are concatenated with the original entropy-based descriptors to form an enriched feature vector that improves classification performance while maintaining interpretability. This strategy avoids reliance on deep learning architectures and provides a transparent way to model higher-order relationships within the feature space.

2.3.6. Final Feature Vector Construction

To improve the separability of the extracted features, we construct a hybrid feature vector by fusing band-specific entropy measures with statistical descriptors derived from the Gram Matrix. This combination allows us to capture both local irregularities and global correlation structures in EEG signals, improving seizure detection performance while maintaining interpretability. The final feature vector X is formed as follows:

$$X = [\text{Entropy features}, \text{Gram matrix features}] \quad (9)$$

This strategy ensures that both **temporal complexity** and **second-order statistical relationships** are encoded in the feature space, leading to more robust discrimination between interictal and ictal EEG segments.

The feature extraction pipeline is summarized as follows:

1. The EEG signal is first decomposed into Beta (12–30 Hz) and Gamma (30–60 Hz) rhythm components using the Discrete Legendre Transform (DLT).
2. Four entropy measures—Approximate Entropy (ApEn), Permutation Entropy (PermEn), Sample Entropy (SampEn), and Fuzzy Entropy (FuzzyEn)—are computed for each rhythm, yielding **8 band-specific features** (4 per band).
3. These 8 features form a vector $F \in R^8$, from which the Gram Matrix is constructed as $G = FF^T$.
4. Four global descriptors—**trace**, **Frobenius norm**, **maximum eigenvalue**, and **determinant**—are extracted from G and concatenated with the original 8 entropy features to form the final **12-dimensional** feature vector (Eq. 9).



Additionally, all features are normalized using z-score normalization to eliminate bias due to scale differences:

$$X_{norm} = \frac{X(i) - \mu}{\sigma} \quad (10)$$

Where μ and σ represent the mean and standard deviation of each feature across the training set.

2.4. Feature Classification

To evaluate the discriminative power of the extracted features, we employ two distinct classification strategies: a Support Vector Machine (SVM) with RBF kernel and a Probabilistic Collaborative Representation-Based Classifier (ProCRC). These models offer complementary advantages in terms of generalization, interpretability, and robustness to inter-subject variability.

2.4.1. Support Vector Machine (SVM)

The Support Vector Machine is a well-established supervised learning algorithm known for its strong generalization performance in high-dimensional spaces [27]. The decision function of SVM is defined as:

$$f(x) = \text{sign}\left(\sum_{i=1}^N \alpha_i y_i K(x, x_i) + b\right) \quad (11)$$

Where α_i represent Lagrange multipliers, $y_i \in \{-1, +1\}$ denote class labels, $K(\cdot, \cdot)$ refers to kernel function, and b denotes the bias term. In this work, an SVM employing a Radial Basis Function (RBF) kernel is utilized to classify EEG segments into interictal (Group D) and ictal (Group E) states. The RBF kernel, often referred to as the Gaussian kernel is given by:

$$K(x_i, x_j) = \exp(-\gamma \|x_i - x_j\|^2) \quad (12)$$

Where x_i and x_j are feature vectors of EEG segments, and γ controls the influence radius of each support vector. This kernel maps the input features into a higher-dimensional space to find an optimal separating hyperplane between interictal and ictal EEG patterns. The RBF kernel was selected due to its ability to handle nonlinear decision boundaries commonly found in biomedical signal classification tasks.

The classification pipeline is implemented using the LIBSVM package [28], which provides an efficient and standardized framework for SVM-based classification tasks. LIBSVM supports multi-class classification, parameter tuning via grid search, and cross-validation strategies, making it suitable for our experimental setup.

2.4.2. Probabilistic Collaborative Representation-Based Classifier (ProCRC)

Collaborative Representation-Based Classification (CRC) assumes that a test sample can be effectively reconstructed using training samples from the same class [29]. In contrast to traditional sparse representation approaches, CRC treats all training samples as a collaborative dictionary, without enforcing sparsity constraints.

The reconstruction error for each class is computed as:

$$E_c = \|y - D_c w_c\|^2 + \lambda \|w_c\|_1 \quad (13)$$

Where y is the test sample, D_c is the sub-dictionary formed by training samples from class c , w_c is the weight vector, and λ controls regularization strength.

In the probabilistic extension (ProCRC), the likelihood of successful reconstruction is estimated based on the distribution of residuals. The test sample is assigned to the class with the highest posterior probability:

$$P(c|y) = \frac{P(y|c)P(c)}{P(y)} \quad (14)$$

This approach enhances robustness against noise and minor morphological variations in EEG signals, making it particularly suitable for seizure detection tasks where subject specific differences are common.

2.5. Performance Evaluation

To evaluate the performance of the proposed seizure detection system, we conduct a comprehensive evaluation using standard classification metrics and cross-validation techniques. We use the following performance measures to evaluate classification quality:

- **Accuracy** — Measures the overall correctness of the classifier.
- **Sensitivity (Recall)** — Rate of correctly detected positive instances.
- **Specificity** — Indicates the model's ability to identify true negative cases.
- **AUC** — Area under the ROC curve, used to evaluate the discriminative power of the model.

These metrics are computed based on the confusion matrix elements:



$$Accuracy = \frac{TP + TN}{TP + TN + FP + FN} \quad (15)$$

$$Sensitivity = \frac{TP}{TP + FN} \quad (16)$$

$$Specificity = \frac{TN}{TN + FP} \quad (17)$$

Where: - **TP**: True Positive - **TN**: True Negative - **FP**: False Positive - **FN**: False Negative.

3. EXPERIMENTAL RESULTS

To ensure a comprehensive and unbiased evaluation of the proposed seizure detection framework, we employed two complementary validation strategies: stratified train/test split and cross-validation. The former allows for straightforward performance comparison with prior studies that use fixed data partitions, while the latter provides a more robust estimation by minimizing variance due to random sampling. This dual-protocol approach offers multiple perspectives on model generalization and strengthens the reliability of the reported results. All experiments were conducted using MATLAB R2022a on an HP EliteBook 8570w equipped with an Intel Core i7-3720QM 2.60 GHz processor and 8 GB RAM. In this section, the proposed processing chain is also compared with several well-known existing approaches.

3.1. Stratified Train/Test Split Strategy

To ensure a fair and reproducible evaluation, we employed a stratified 60–40 train/test split for both the Bonn University and Hauz Khas (HK) EEG datasets. For the Bonn dataset, 120 segments (60 D + 60 E) were used for training and 80 (40 D + 40 E) for testing. For the HK dataset, which contains 50 interictal and 50 ictal segments, we used 60 samples (30 interictal + 30 ictal) for training and 40 (20 interictal + 20 ictal) for testing, preserving perfect class balance in both cases.

During training, 10-fold cross-validation was applied to optimize hyperparameters (e.g., SVM's kernel width γ and regularization parameter C), ensuring robustness against overfitting and random partitioning effects.

As summarized in Table 1, both SVM and ProCRC achieved 100% accuracy, sensitivity, and specificity on the Bonn D–E task, indicating perfect separation of interictal activity from the epileptogenic zone (Group D) and ictal seizure activity (Group E). On the independent HK dataset, the same pipeline yielded 97.5% accuracy, with 95.0% sensitivity and 100% specificity for both classifiers, confirming strong generalization across acquisition protocols and patient populations.

Fig. 4 displays the confusion matrices for all four combinations: Bonn (D–E) and HK (interictal–ictal), each classified using SVM and ProCRC. Fig. 5 presents the ROC curves along with their respective AUC scores for SVM and ProCRC classifiers for Bonn dataset.

To evaluate the generalization capability of the proposed method across diverse brain states, additional classification experiments were conducted on multiple subset combinations of the Bonn EEG dataset, encompassing both binary and potential multi-class scenarios. The results, summarized in Table 2, highlight the effectiveness and robustness of the entropy-Gram feature representation in capturing discriminative patterns across different neurological conditions. Furthermore, to assess cross-dataset scalability, we extended the evaluation to the Hauz Khas (HK) dataset, including both binary (preictal vs. ictal) and three-class (preictal vs. interictal vs. ictal) tasks, the corresponding results are reported in the same table.

3.2. Cross Validation Strategy

To ensure robustness and minimize bias due to random data partitioning, 10-fold cross-validation was employed for both the Bonn University and Hauz Khas (HK) datasets. In this procedure, each dataset was randomly divided into 10 equal-sized folds; the model was trained on 9 folds and evaluated on the remaining fold. This process was repeated 10 times, with each fold serving once as the test set. The final performance was reported as the mean accuracy across all folds, providing a statistically stable estimate of generalization capability. The results are summarized in Table 3 and visualized in Fig. 6.

For the Bonn dataset (Groups D vs. E), the mean classification accuracy was 99.5% for ProCRC and 98.5% for SVM (Fig. 6(a), Table 3). For the HK dataset (interictal vs. ictal), the proposed pipeline, applied, achieved 97% (ProCRC) and 96% (SVM), respectively (Fig. 6(b), Table 3). These results confirm that the entropy-Gram feature representation generalizes well across independent clinical datasets, even under rigorous cross-validation.



3.3. Comparative Performance with Existing Methods

To rigorously evaluate the proposed framework, we conduct a comparative analysis on two independent EEG datasets: the Bonn University dataset and the Hauz Khas (HK) dataset. This dual-dataset validation ensures both methodological soundness and clinical generalizability.

3.3.1. Comparative Analysis on the Bonn Dataset

To evaluate the efficacy of the proposed seizure detection framework, we benchmark our results against multiple state-of-the-art approaches reported in the literature. The comparison was carried out on the same Bonn University EEG dataset (Groups D and E), under identical preprocessing conditions to ensure fair evaluation. Table 4 summarizes the classification accuracy of each approach. As presented in Table 4, the method proposed by Alzamili et al. [30] achieved a classification accuracy of 100% based on Ruzicka similarity analysis. In their approach, EEG segments were partitioned into fixed-size blocks (e.g., 5, 10, and 15 samples), and feature selection was performed by measuring inter-block similarity to identify dominant patterns. The selected features were then used to train traditional classifiers for seizure detection.

While this method demonstrated high performance, it relied on manual block sizing and assumed stationarity within each segment, limitations that may affect generalization across different EEG morphologies and patient populations. In contrast, our approach employed band-limited entropy features combined with Gram matrix modeling to capture both local irregularities and global correlations without requiring arbitrary segmentation or GPU-based training.

In [31], a wavelet-based framework was proposed for multi-resolution seizure detection. The method employed DWT to decompose EEG signals into multiple sub-bands, from which both temporal and spectral features were extracted. Temporal features such as minimum amplitude, mean amplitude, and standard deviation were computed for each sub-band to characterize time-domain variations. Additionally, Power Spectral Density (PSD)-based descriptors — including maximum PSD, mean PSD, and variance of PSD — were used to model non-stationary and nonlinear properties of EEG activity. However, this approach required multi-level decomposition and extensive parameter tuning, which increased computational load and made the pipeline more sensitive to noise and signal quality. In contrast, our framework extracts band-limited entropy features and applies Gram matrix modeling in a single step, significantly reducing preprocessing complexity while preserving high discriminative capability.

In [32], the performance of various machine learning and deep learning models for automated epileptic seizure recognition was evaluated. Several conventional ML and DL algorithms—including SVM, Logistic Regression, k-Nearest Neighbors (KNN), Artificial Neural Network (ANN), and Long Short-Term Memory (LSTM)—were implemented to assess their effectiveness in classifying EEG signals. The proposed LSTM-based model was trained for learning temporal relationships within EEG data, and a comparative analysis was conducted across all methods. The results showed that the LSTM achieved a validation accuracy of 97%, outperforming other algorithms in terms of classification precision. This superior performance was attributed to the ability of LSTM networks to model sequential structures and long-range correlations in EEG signals, which is essential for detecting dynamic changes during seizure events.

In comparison, traditional ML classifiers relied on handcrafted features and did not completely utilize the temporal structure of the input data. However, it was observed that LSTM required longer training time and higher computational resources compared to shallow ML models. This suggests that while LSTM achieves high accuracy, its deployment in real-time or resource-constrained settings may be limited.

Malekzadeh et al. [33]-[34], investigated epileptic seizure detection on the Bonn dataset using two distinct wavelet-based pipelines. In their first study, the Tunable-Q Wavelet Transform (TQWT) was applied to decompose EEG signals into multiple sub-bands, from which statistical and nonlinear features were extracted and fed to shallow classifiers (e.g., SVM, k-NN). Under optimal parameter tuning, this approach yielded classification accuracies in the range of 96.71% to 98.82% for the interictal (D) vs. ictal (E) task.

In a follow-up work, the same group introduced a more advanced framework combining Dual-Tree Complex Wavelet Transform (DT-CWT) with fractal-dimension descriptors and mRMR-based feature selection, followed by a convolutional autoencoder (CNN-AE) for representation learning and classification. This deeper architecture achieved 99.74% accuracy on the same D–E binary task, demonstrating the benefit of representation learning, albeit at the cost of increased model complexity and reduced interpretability.

Wang et al. [35] proposed an automated epilepsy diagnosis system based on multi-domain features and nonlinear EEG signal analysis. In their study, time-domain, frequency-domain, and time-frequency features were combined with entropy-based nonlinear descriptors to enhance seizure detection performance. EEG signals were preprocessed using wavelet thresholding to suppress noise and artifacts. Subsequently, features were extracted from five clinically relevant frequency sub-bands and reduced using Principal Component Analysis along with analysis of variance. The selected feature set was evaluated with multiple classifiers, among which SVM reached the peak classification accuracy of 99.25% under cross-validation strategy protocol.

An automated framework for detecting epileptic seizures was additionally proposed by Hassan et al. [36], based on signal decomposition and statistical modeling. In their work, the EEG signals were decomposed into



Intrinsic Mode Functions (IMFs) using the Complete Ensemble Empirical Mode Decomposition with Adaptive Noise (CEEMDAN) method, capturing oscillatory patterns across multiple temporal scales. The IMFs were characterized using the Normal Inverse Gaussian (NIG) probability density function, providing a parametric representation of each mode. This feature extraction strategy was combined with an Adaptive Boosting (AdaBoost) classifier to distinguish between seizure and nonseizure EEG segments. Classification results reported an accuracy of 99%, confirming the efficiency of CEEMDAN–NIG in identifying seizure-related patterns.

Molla et al. [37] introduced an automated seizure detection framework based on multi-scale entropy features and graph eigen decomposition (GED) for feature selection. In their approach, EEG signals were first segmented into short time windows to capture localized dynamics. Each segment was then decomposed using the Discrete Wavelet Transform (DWT) into multiple subbands. From each subband, several entropy-based features—such as Approximate Entropy (ApEn), Permutation Entropy (PermEn), and Sample Entropy (SampEn)—were extracted alongside spike-related descriptors, forming a high-dimensional feature vector. To reduce redundancy and improve discriminative power, a Graph Eigen Decomposition (GED)-based feature selection method was applied. This ensured that only the most informative features were retained for classification. Finally, a Feedforward Neural Network (FfNN) was employed to classify the selected features as seizure or non-seizure. Experimental results showed a classification accuracy of 98.6%.

3.3.2. Comparative Analysis on the Hauz Khas (HK) Dataset

To assess generalizability beyond the canonical Bonn benchmark, we evaluated the proposed framework on the independent Hauz Khas (HK) EEG dataset, which comprises clinically recorded interictal and ictal segments. The performance comparison with existing methods on the Hauz Khas dataset is summarized in Table 5.

A recent study by Wang et al. [38] also evaluated performance on the Hauz Khas dataset using a multimodal dual-stream neural network that integrates 1D-CNN (for temporal features), 2D-CNN (for spatial features from STFT spectrograms), and LSTM (for long-range dependencies), enhanced with channel attention. Their approach achieved 97.5% accuracy, matching our result, yet relied on high-end computational hardware and offered no mechanism for interpreting why a decision was made. In contrast, our pipeline attains identical accuracy using only 12 handcrafted, physiologically grounded features (entropy + Gram descriptors) and lightweight classifiers (SVM/ProCRC), running efficiently on a standard laptop without GPU acceleration, demonstrating that clinical-grade performance need not entail black-box complexity or prohibitive hardware demands.

Panda et al. [39] employed an ensemble of four deep neural networks (DNNs) with a multilayer perceptron (MLP) as meta-classifier, trained on 10 statistical features (5 time-domain: skewness, kurtosis, Hjorth parameters; 5 frequency-domain: AM/FM bandwidths, spectral entropy, power, centroid) extracted from Empirical Wavelet Transform (EWT)-decomposed EEG sub-bands, and reported 97.0% accuracy for the interictal–ictal classification task.

In the context of interictal–ictal classification on the Hauz Khas dataset, Dash et al. [40] utilized a hybrid signal-processing pipeline combining wavelet packet decomposition (Daubechies-2, level 2) and dynamic mode decomposition (DMD) to derive four statistical descriptors—power spectral density (PSD), variance, Katz fractal dimension (KFD), and DMD power, and achieved 96.5% accuracy with SVM (RBF kernel) and 96.0% with KNN ($k = 5$) under a 60–40 train/test split.

Sheng et al. [41] proposed a Deep Knowledge-Driven TSK Fuzzy Classifier (DKD-TSK-FC) for EEG-based epilepsy diagnosis, where a 1D-CNN serves as the teacher model and a first-order Takagi–Sugeno–Kang fuzzy classifier acts as the student. Knowledge distillation was used to transfer soft-label knowledge from the teacher to the student, while preserving interpretability. Evaluated on the Hauz Khas dataset for the interictal vs. ictal classification task (Task 5), the method achieved an accuracy of 98.76%, outperforming its teacher (1D-CNN: 97.67%) and conventional TSK variants (e.g., FCM-TSK-FC: 90.47%, PCA-TSK-FC: 91.34%).

Gupta et al. [42] employed a signal modeling approach based on multirate DCT filterbanks to decompose EEG into five brain rhythms (Delta, Theta, Alpha, Beta, Gamma), followed by statistical modeling of these rhythms as fractional Brownian motion (fBm) and fractional Gaussian noise (fGn) processes. The Hurst exponent and ARMA parameters were used as features, and an SVM with RBF kernel achieved 96.5% accuracy for the interictal–ictal classification task on the Hauz Khas dataset.

Jebaraj and Elango [43] proposed TemporalSNN, a lightweight spiking neural network optimized for neuromorphic hardware. Their pipeline combined comprehensive feature extraction (230 time/frequency/nonlinear/wavelet features) with mutual information (MI)-based feature selection to reduce dimensionality. Evaluated on the HAUZ (Hauz Khas) dataset for binary interictal–ictal classification, their method improved accuracy from 77.2% (without feature selection) to 92.5% (with 75% feature reduction). The approach emphasized low computational complexity and robustness, making it suitable for real-time, resource-constrained deployment.



3.4. Comparative Analysis of Frequency Bands

To validate the choice of Beta (12–30 Hz) and Gamma (30–60 Hz) frequency bands, we conducted additional experiments using Delta (0.5–4 Hz) and Theta (4–8 Hz) components, extracted via the same DLT–entropy–Gram pipeline. As shown in Table 6, classification performance drops significantly in the low-frequency range, ProCRC achieves 92.5% accuracy, compared to 100% in Beta–Gamma bands.

This result supports the neurophysiological rationale for prioritizing high-frequency bands: while ictal EEG is often dominated by slow waves, the transition to seizure involves localized cortical hyper-synchronization in the β – γ range, a more stable and discriminative signature for automated detection.

4. DISCUSSION

The exceptional performance of the entropy–Gram framework, even on short, single-channel segments, suggests that epileptic transitions are more reliably encoded in signal irregularity and feature interdependence than in raw amplitude or spectral power alone. This aligns with growing evidence that high-frequency cortical synchronization (e.g., in β – γ bands) reflects early ictogenesis [18], while Gram-based modeling captures how entropy features co-vary across frequency bands, a signature often missed by flat feature vectors. Crucially, this representation requires no deep learning, yet achieves 100% accuracy on the Bonn dataset, indicating that interpretability and performance need not be traded off.

ProCRC’s consistent edge over SVM (99.5% vs. 98.5% in cross-validation) likely stems from its probabilistic collaborative reconstruction mechanism, which is inherently more robust to intra-class morphological variability, a hallmark of EEG across patients. Unlike SVM’s margin-based decision boundary, ProCRC evaluates how well a test sample can be reconstructed using training samples from each class, making it less sensitive to outliers (e.g., transient artifacts in interictal segments).

The results on the independent Hauz Khas dataset (97.5%) confirm generalizability beyond Bonn’s controlled setting, though the slight accuracy drop highlights sensitivity to recording conditions (e.g., noise, montage). Importantly, performance remains high without fine-tuning, suggesting the feature space is domain-agnostic at the representational level. However, this robustness does not imply suitability for all clinical scenarios: the method assumes clear interictal/ictal boundaries and may require adaptation for long-term monitoring where seizure evolution is gradual.

While our framework does not outperform all deep learning methods in raw accuracy, it achieves competitive performance with full interpretability and minimal computational overhead. This trade-off may be advantageous in applications where understanding why a decision was made is as important as the decision itself.

5. LIMITATIONS OF THE STUDY

Despite the strong performance and interpretability of the proposed framework, several limitations should be acknowledged. First, the evaluation was conducted on short, single-channel EEG segments from controlled laboratory settings (Bonn) and a small clinical dataset (Hauz Khas). While this enables reproducibility and benchmarking, it may not fully reflect the complexity of long-term, multi-channel, real-world recordings, where artifacts, non-stationarities, and inter-channel dynamics (e.g., coherence, network connectivity) play a critical role. Second, the datasets used, though well-established, have limited sample size and demographic diversity compared to large-scale clinical repositories, potentially constraining the statistical generalizability of the results. Third, the current implementation is offline and segment-based, without support for real-time streaming, temporal seizure evolution modeling, or patient-specific adaptation, key requirements for clinical deployment. Finally, while the entropy–Gram feature set is robust across two datasets, its behavior may vary with different acquisition systems, noise profiles, or electrode montages, necessitating further validation in heterogeneous clinical environments. Addressing these limitations, through multi-channel extensions, real-time optimization, and large-scale cross-center studies, constitutes a natural direction for future work.

6. FUTURE WORK

Future research directions include extension to multichannel EEG analysis, integration of lightweight recurrent networks for enhanced temporal modeling, implementation in real-time monitoring systems for long-term seizure prediction, and exploration of fractal dimension (e.g., Higuchi’s FD) to further capture scale-invariant properties of epileptic EEG signals. Ultimately, this line of work aims to demonstrate that structured feature extraction and classification can achieve reliable seizure detection without the complexity of deep learning architectures.

7. CONCLUSION

This paper presented an interpretable and efficient framework for automated epileptic seizure detection based on band-limited entropy features and Gram matrix modeling. By employing the Discrete Legendre Transform,



Beta and Gamma frequency components were extracted in a single decomposition step, followed by entropy-based characterization and second-order statistical enhancement through Gram matrices. Experimental evaluations on the Bonn University EEG dataset demonstrated an average accuracy of 99.5% under 10-fold cross-validation and 100% under a stratified train/test split, while validation on the independent Hauz Khas clinical dataset achieved accuracies of 97% and 97.5%, respectively. Unlike deep learning-based approaches, the proposed method remains lightweight, transparent, and free from extensive training or hardware requirements, making it suitable for practical clinical and portable diagnostic applications. Furthermore, the explicit feature construction and matrix-based representation facilitate reproducibility and allow clinicians to interpret seizure-related dynamics beyond black-box predictions. These characteristics highlight the potential of the proposed framework as a reliable and deployable solution for real-world seizure monitoring scenarios where efficiency, transparency, and robustness are essential.

Data Availability.

The EEG data used in this study are publicly available:

- The Bonn University EEG dataset can be accessed via the UCI Machine Learning Repository: <https://www.ukbonn.de/en/epileptology/workgroups/lehnertz-workgroup-neurophysics/downloads>.
 - The Hauz Khas (HK) EEG dataset is available at: https://www.researchgate.net/publication/308719109_EEG_Epilepsy_Datasets.
- Both datasets are freely accessible for academic research with no usage restrictions.

Funding. There is no funding for this work.

Conflicts of interest. The authors declare no conflict of interest.

Ethics. The authors declare that the present research work has fulfilled all relevant ethical guidelines required by [COPE](#).

REFERENCES

- [1] M. Khaksar, A. Golrou, and S. Rahati-Ghuchani, "Automatic recognition of sleep spindles based on two-stage classifier with artificial neural networks and support vector machines," *Majlesi Journal of Electrical Engineering*, vol. 2, no. 1, pp. 83–90, 2009. doi: 10.1234/mjee.v2i1.45.
- [2] M. Vaezi and M. Nasri, "Sleep stage classification using Laplacian score feature selection method by single channel EEG," *Majlesi Journal of Electrical Engineering*, vol. 14, no. 4, 2020. doi: 10.29252/mjee.14.4.11.
- [3] A. Tobieha, N. Behzadfar, M. R. Yousefi, H. Mahdavi-Nasab, and G. Shahgholian, "Analysis of the changes in the distinguishing features in electroencephalogram signal processing for heroin addicts," *Majlesi Journal of Electrical Engineering*, vol. 19, no. 1, pp. 1–13, Mar. 2025. doi: 10.57647/j.mjee.2025.1901.14.
- [4] M. Mabrouk, "Non-invasive EEG-based BCI system for left or right hand movement," *Majlesi Journal of Electrical Engineering*, vol. 5, no. 3, 2024. Available: <https://oicpress.com/mjee/article/view/5180>.
- [5] E. Wirrell, P. Tinuper, E. Perucca, and S. L. Moshé, "Introduction to the epilepsy syndrome papers," *Epilepsy Research*, vol. ---, pp. 1330–1332, 2022. doi: 10.1111/epi.17262.
- [6] C. Baumgartner, J. Baumgartner, C. Lang, T. Lisy, and J. P. Koren, "Seizure detection devices," *Journal of Clinical Medicine*, vol. 14, no. 3, p. 863, 2025. doi: 10.3390/jcm14030863.
- [7] V. Rasoulzadeh, E. Erkus, T. Yogurt, I. Ulusoy, and S. A. Zergeroğlu, "A comparative stationarity analysis of eeg signals," *Annals of Operations Research*, vol. 258, pp. 133–157, 2017. doi: 10.1007/s10479-016-2187-3.
- [8] P. Baghaie-Anaraki, M. Yazdchi, and A. Karimian, "EEG pattern recognition to diagnose epilepsy using wavelet and chaos transformations," *Majlesi Journal of Electrical Engineering*, vol. 2, no. 1, pp. 51–59, 2008. doi: 10.1234/mjee.v2i1.41.
- [9] N. Kannathal, M. L. Choo, U. R. Acharya, and P. Sadasivan, "Entropies for detection of epilepsy in EEG," *Computer methods and programs in biomedicine*, vol. 80, no. 3, pp. 187–194, 2005. doi: 10.1016/j.cmpb.2005.06.012.
- [10] Y. Zhang, L. Wang, and H. Chen, "A low-complexity seizure detection algorithm for ultra-low power wearable devices," *IEEE Transactions on Biomedical Circuits and Systems*, vol. 17, no. 2, pp. 230–239, 2023. doi: 10.1109/ACCESS.2023.3235913



- [11] B. S. Nanthini and B. Santhi, "Electroencephalogram signal classification for automated epileptic seizure detection using genetic algorithm," *Journal of natural science, biology, and medicine*, vol. 8, no. 2, p. 159, 2017. doi: 10.4103/jnsbm.jnsbm_285_16.
- [12] A. Şengür, Y. Guo, and Y. Akbulut, "Time–frequency texture descriptors of eeg signals for efficient detection of epileptic seizure," *Brain Informatics*, vol. 3, pp. 101–108, 2016. doi: 10.1007/s40708-015-0029-8.
- [13] N. Sairamy, S. Thomas George, D. Narain Ponraj, and M. Subathra, "Automated detection of epileptic seizure using histogram of oriented gradients for analysing time frequency images of eeg signals," in *Smart and Innovative Trends in Next Generation Computing Technologies: Third International Conference, NGCT 2017, Dehradun, India, October 30-31, 2017, Revised Selected Papers, Part II 3*. Springer, 2018, pp. 932–943. doi: 10.1007/978-981-10-8660-1_71.
- [14] M. Yusaf, R. Nawaz, and J. Iqbal, "Robust seizure detection in eeg using 2D DWT of time-frequency distributions," *Electronics Letters*, vol. 52, no. 11, pp. 902–903, 2016. doi: 10.1049/el.2016.0630.
- [15] J. Mutersbaugh, V. Lam, M. G. Linguraur, and S. M. Anwar, "Epileptic seizure classification using multidimensional EEG spectrograms," in *2023 19th International Symposium on Medical Information Processing and Analysis (SIPAIM)*. IEEE, 2023, pp. 1–4. doi: 10.1109/SIPAIM56729.2023.10373429.
- [16] W. Zeng, L. Shan, B. Su, and S. Du, "Epileptic seizure detection with deep EEG features by convolutional neural network and shallow classifiers," *Frontiers in neuroscience*, vol. 17, p. 1145526, 2023. doi: 10.3389/fnins.2023.1145526.
- [17] Q. Xin, S. Hu, S. Liu, L. Zhao, and Y.-D. Zhang, "An attention-based wavelet convolution neural network for epilepsy EEG classification," *IEEE Transactions on Neural Systems and Rehabilitation Engineering*, vol. 30, pp. 957–966, 2022. doi: 10.1109/TNSRE.2022.3166181.
- [18] E. Boran, J. Sarnthein, N. Krayenbühl, G. Ramantani, and T. Fedele, "High-frequency oscillations in scalp EEG mirror seizure frequency in pediatric focal epilepsy," *Scientific Reports*, vol. 9, no. 1, p. 16560, 2019. doi: 10.1038/s41598-019-52700-w.
- [19] R. G. Andrzejak, K. Lehnertz, F. Mormann, C. Rieke, P. David, and C. E. Elger, "Indications of nonlinear deterministic and finite-dimensional structures in time series of brain electrical activity: Dependence on recording region and brain state," *Physical Review E*, vol. 64, no. 6, p. 061907, 2001. doi: 10.1103/PhysRevE.64.061907.
- [20] R. Sharma, P. K. Gupta, and M. K. Verma, "EEG Epilepsy Datasets," *ResearchGate*, 2016. doi: 10.13140/RG.2.2.14280.32006.
- [21] L. C. D. Nkengfack, D. Tchiotso, R. Atangana, V. Louis-Door, and D. Wolf, "EEG signals analysis for epileptic seizures detection using polynomial transforms, linear discriminant analysis and support vector machines," *Biomedical Signal Processing and Control*, vol. 62, p. 102141, 2020. doi: 10.1016/j.bspc.2020.102141.
- [22] S. M. Pincus, "Approximate entropy as a measure of system complexity," *Proceedings of the National Academy of Sciences*, vol. 88, no. 6, pp. 2297–2301, 1991. doi: 10.1073/pnas.88.6.2297.
- [23] C. Bandt and B. Pompe, "Permutation entropy: a natural complexity measure for time series," *Physical Review E*, vol. 66, no. 2, p. 025701, 2002. doi: 10.1103/PhysRevLett.88.174102.
- [24] J. S. Richman and J. R. Moorman, "Sample entropy," *American Journal of Physiology-Heart and Circulatory Physiology*, vol. 286, no. 6, pp. H2503–H2508, 2004. doi: 10.1016/S0076-6879(04)84011-4.
- [25] Al-Sharhan, Salah, Fakhri Karray, Wail Gueaieb, and O. Basir. "Fuzzy entropy: a brief survey." In *10th IEEE international conference on fuzzy systems.(Cat. No. 01CH37297)*, vol. 3, pp. 1135-1139. IEEE, 2001. doi: 10.1109/FUZZ.2001.1008855.
- [26] L. A. Gatys, A. S. Ecker, and M. Bethge, "A neural algorithm of artistic style," *arXiv preprint arXiv:1508.06576*, 2015. doi: 10.48550/arXiv.1508.06576.
- [27] M. A. Hearst, S. T. Dumais, E. Osuna, J. Platt, and B. Schölkopf, "Support vector machines," *IEEE Intell. Syst.*, vol. 13, no. 4, pp. 18–28, 1998. doi: 10.1109/5254.708428.
- [28] C.-C. Chang and C.-J. Lin, "Libsvm: A library for support vector machines," *ACM Transactions on Intelligent Systems and Technology*, vol. 2, no. 3, pp. 1–39, 2011. doi: 10.1145/1961189.1961199.



- [29] S. Cai, L. Zhang, W. Zuo, and X. Feng, "A probabilistic collaborative representation based approach for pattern classification," in *Proceedings of the IEEE conference on computer vision and pattern recognition*, 2016, pp. 2950–2959. doi: 10.1109/2FCVPR.2016.322.
- [30] S. L. Alzamili, S. S. Baawi, M. N. Kadhim, D. Al-Shammary, and A. Ibaida, "Efficient feature selection based on ruzicka similarity for eeg diagnosis," *International Journal of Information Technology*, pp. 1–15, 2025. doi: 10.1007/s41870-025-02572-3.
- [31] Aayasha, M. B. Qureshi, M. Afzaal, M. S. Qureshi, and M. Fayaz, "Machine learning-based EEG signals classification model for epileptic seizure detection," *Multimedia Tools and Applications*, vol. 80, no. 12, pp. 17 849–17 877, 2021. doi: 10.1007/s11042-021-10597-6.
- [32] P. Kunekar, M. K. Gupta, and P. Gaur, "Detection of epileptic seizure in eeg signals using machine learning and deep learning techniques," *Journal of Engineering and Applied Science*, vol. 71, no. 1, p. 21, 2024. doi: 10.1186/s44147-023-00353-y.
- [33] A. Malekzadeh, A. Zare, M. Yaghoobi, H. R. Kobravi, and R. Alizadehsani, "Epileptic seizures detection in EEG signals using fusion handcrafted and deep learning features," *Sensors*, vol. 21, no. 22, p. 7710, 2021. doi: 10.3390/s21227710.
- [34] A. Malekzadeh, A. Zare, M. Yaghoobi, and R. Alizadehsani, "Automatic diagnosis of epileptic seizures in EEG signals using fractal dimension features and convolutional autoencoder method," *Big Data and Cognitive Computing*, vol. 5, no. 4, p. 78, 2021.
- [35] L. Wang, W. Xue, Y. Li, M. Luo, J. Huang, W. Cui, and C. Huang, "Automatic epileptic seizure detection in EEG signals using multi-domain feature extraction and nonlinear analysis," *Entropy*, vol. 19, no. 6, p. 222, 2017. doi: 10.3390/e19060222.
- [36] A. R. Hassan, A. Subasi, and Y. Zhang, "Epilepsy seizure detection using complete ensemble empirical mode decomposition with adaptive noise," *Knowledge-Based Systems*, vol. 191, p. 105333, 2020. doi: 10.1016/j.knsys.2019.105333.
- [37] M. K. I. Molla, K. M. Hassan, M. R. Islam, and T. Tanaka, "Graph eigen decomposition-based feature-selection method for epileptic seizure detection using electroencephalography," *Sensors*, vol. 20, no. 16, p. 4639, 2020. doi: 10.3390/s20164639.
- [38] B. Wang, Y. Xu, S. Peng, H. Wang, and F. Li, "Detection method of epileptic seizures using a neural network model based on multimodal dual-stream networks," *Sensors*, vol. 24, no. 11, p. 3360, 2024. doi: 10.3390/s24113360.
- [39] S. Panda, A. Das, S. Mishra, and M. N. Mohanty, "Epileptic seizure detection using deep ensemble network with empirical wavelet transform," *Measurement Science Review*, vol. 21, no. 4, pp. 110–116, 2021. doi: 10.2478/msr-2021-0016.
- [40] D. P. Dash, M. H. Kolekar, and K. Jha, "Surface EEG based epileptic seizure detection using wavelet based features and dynamic mode decomposition power along with KNN classifier," *Multimedia Tools and Applications*, vol. 81, no. 29, pp. 42057–42077, 2022. doi: 10.1007/s11042-021-11487-7.
- [41] G. Sheng, X. Hu, H. Wu, J. Zhu, and P. Shi, "Deep knowledge-driven TSK fuzzy classifier for EEG-based epilepsy diagnosis," *J. Mech. Med. Biol.*, vol. 25, no. 08, p. 2540072, 2025. doi: 10.1142/S021951942540072X.
- [42] A. Gupta, P. Singh, and M. Karlekar, "A novel signal modeling approach for classification of seizure and seizure-free EEG signals," *IEEE Transactions on Neural Systems and Rehabilitation Engineering*, vol. 26, no. 5, pp. 925–935, 2018. doi: 10.1109/TNSRE.2018.2818123.
- [43] G. S. Jebaraj and K. Elango, "EEG seizure classification with temporal spiking neural networks and mutual information-based feature selection," *Journal of Engineering and Applied Science*, vol. 72, no. 1, p. 218, 2025. doi: 10.1186/s44147-025-00796-5.



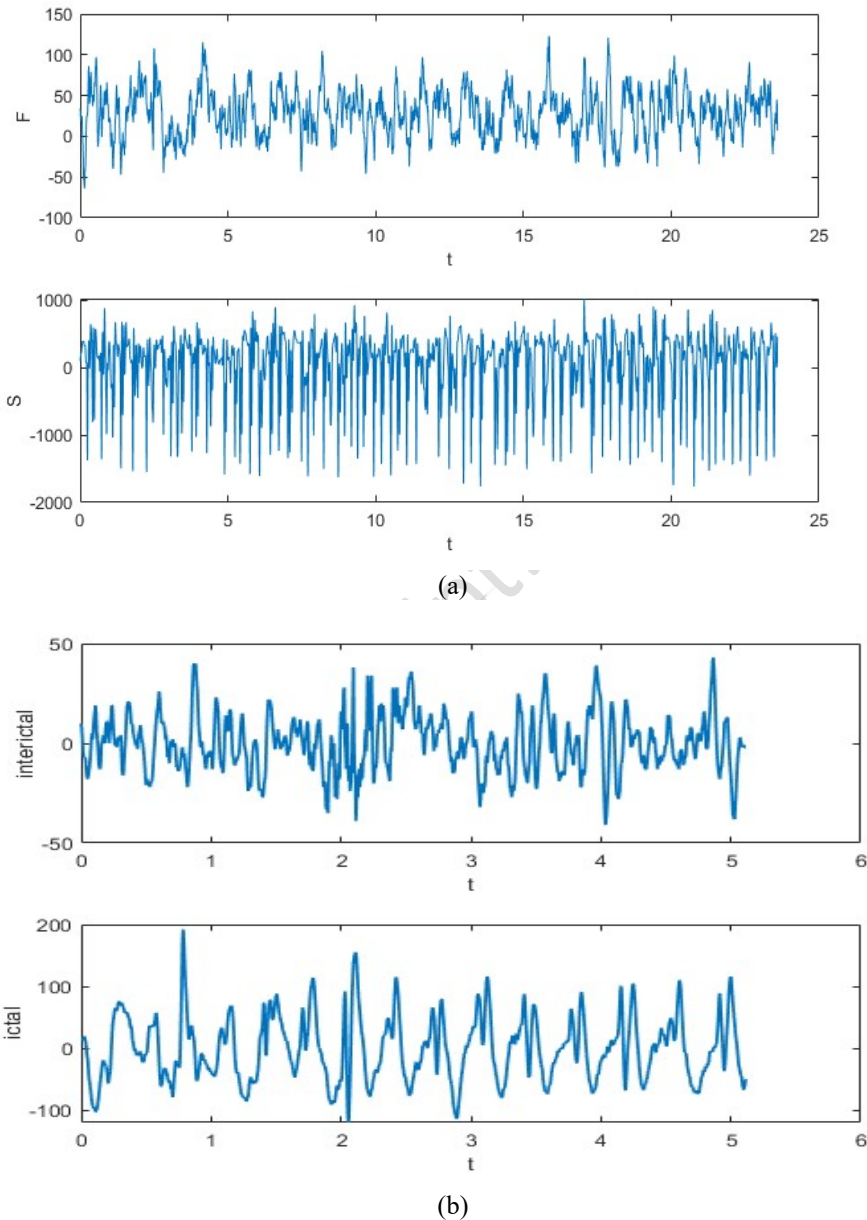


Fig. 1. Sample EEG segments from the Bonn University dataset (a) and the Hauz Khas (HK) dataset (b). In both subfigures, the top row shows interictal EEG activity (Group D:F in Bonn; interictal phase in HK), while the bottom row shows ictal (seizure) EEG activity (Group E:S in Bonn; ictal phase in HK).

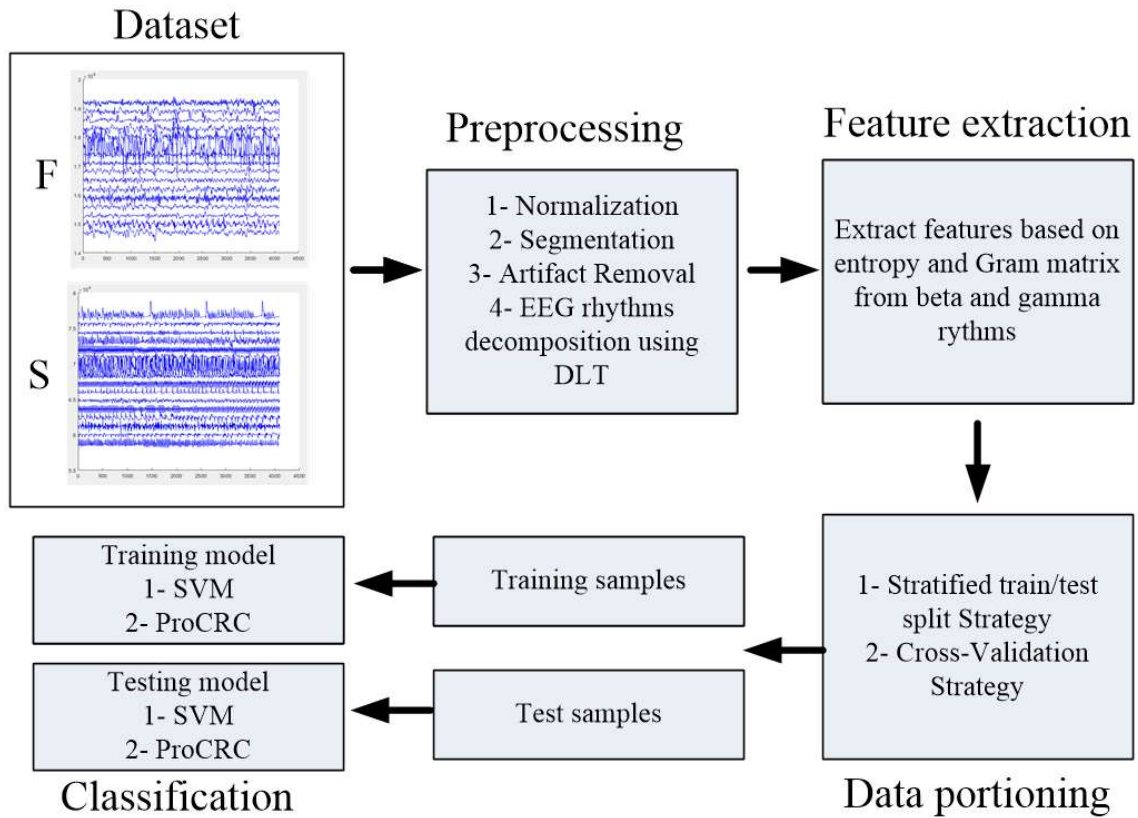


Fig. 2. Overview of the proposed automated seizure detection framework. The pipeline includes preprocessing, band-specific entropy extraction, Gram matrix modeling, and classification using ProCRC and SVM.

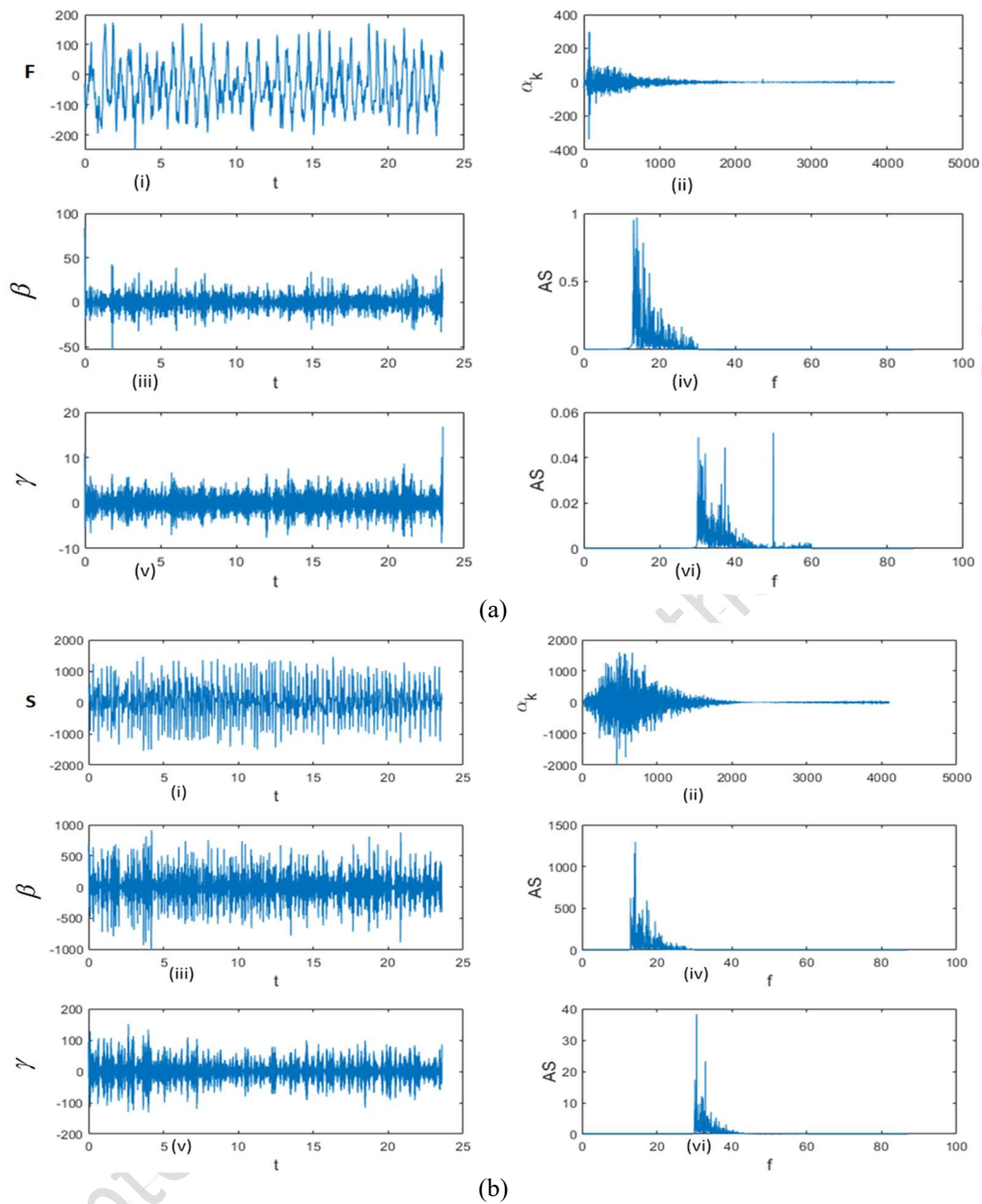


Fig. 3. Extraction of Beta (β : 12–30 Hz) and Gamma (γ : 30–60 Hz) rhythms from (a) interictal EEG (Group D:F) and (b) ictal EEG (Group E:S). (i) Raw EEG signal, (ii) projection coefficients obtained via Discrete Legendre Transform (DLT), (iii) extracted β rhythm, (iv) amplitude spectrum (AS) of β component, (v) extracted γ rhythm, and (vi) amplitude spectrum of γ component.

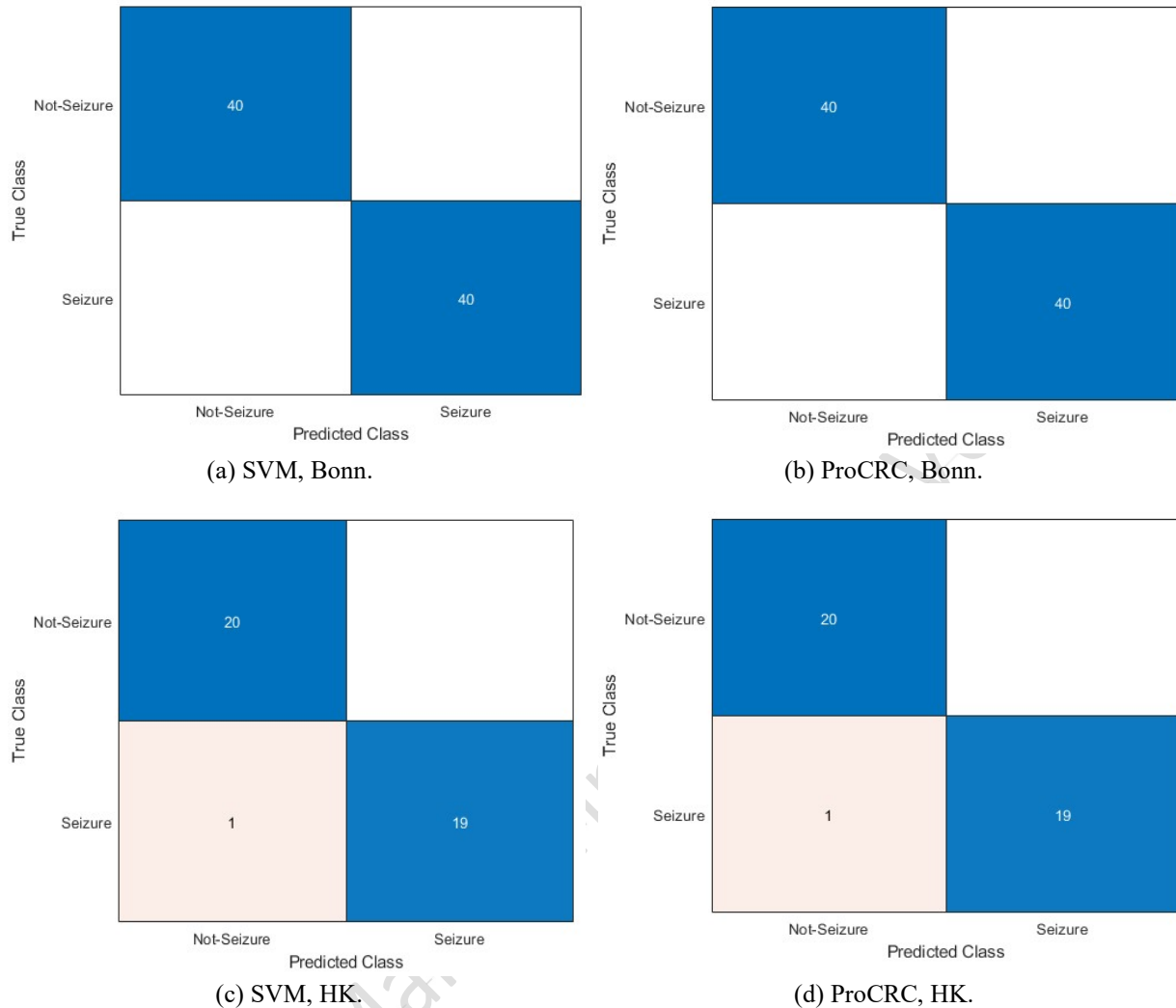


Fig. 4. Confusion matrices of SVM and ProCRC classifiers on the Bonn University dataset (Group D vs. Group E) and the Hauz Khas (HK) dataset (interictal vs. ictal).

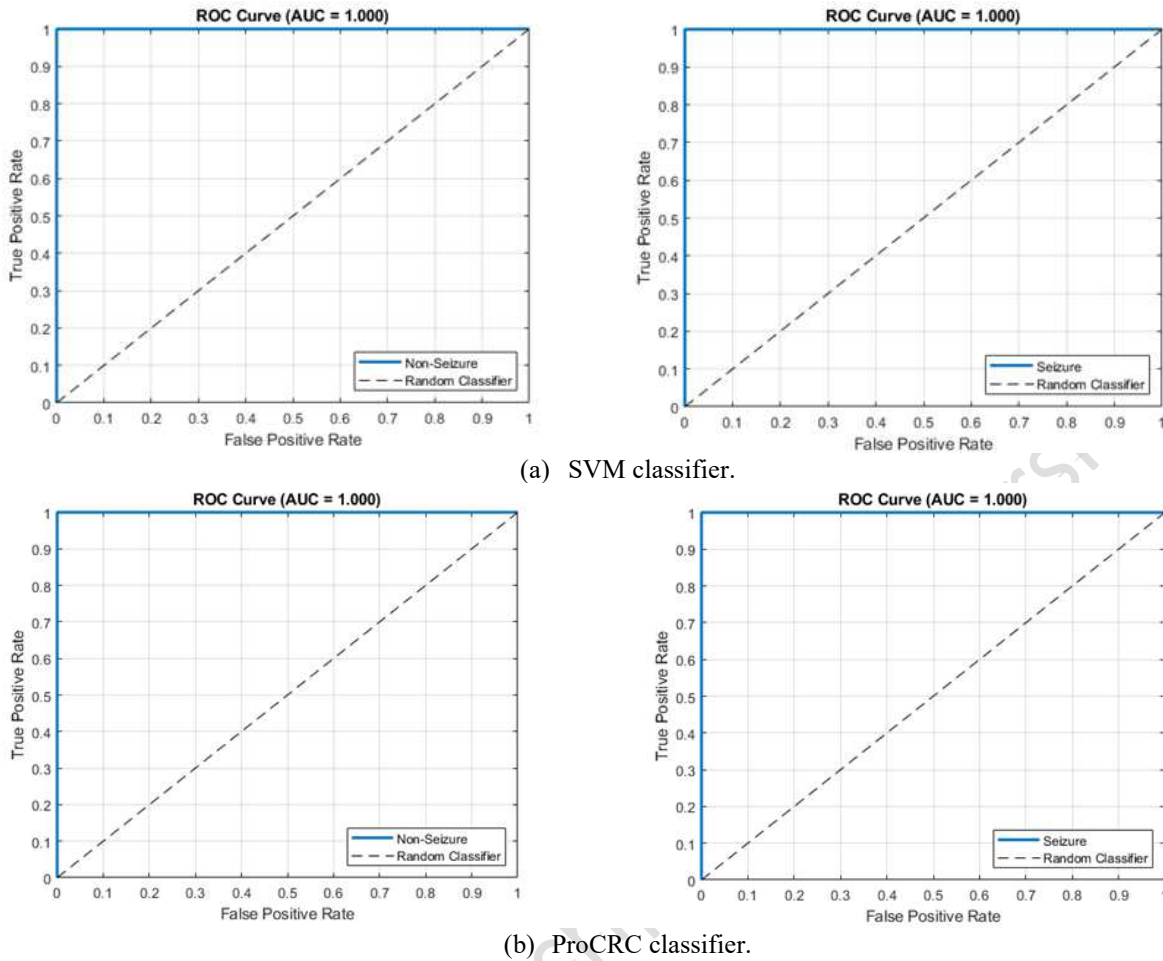


Fig. 5. ROC curves and AUC values for SVM and ProCRC classifiers for non-seizure and seizure categories of Bonn dataset.

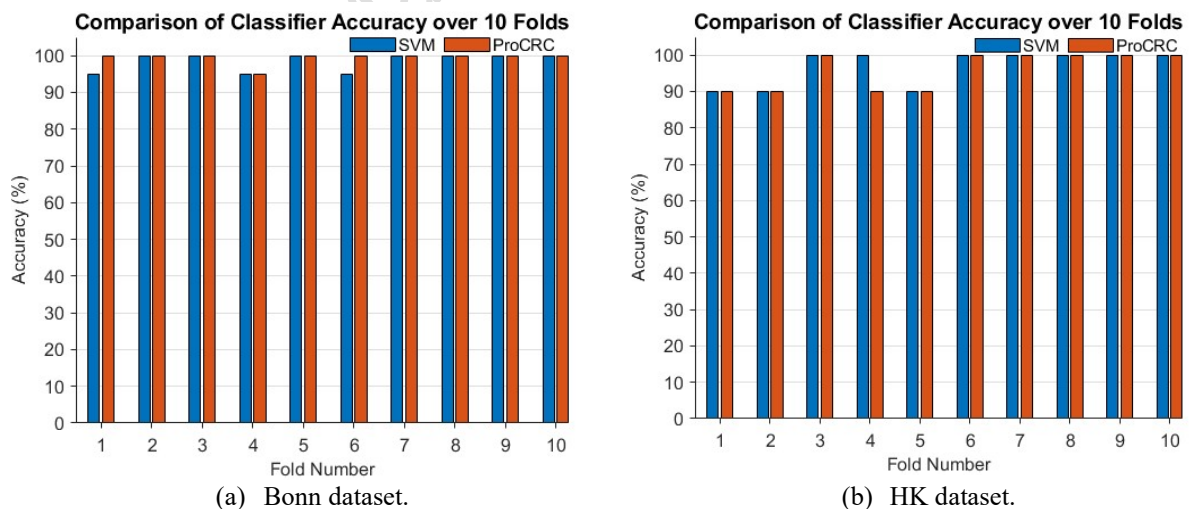


Fig. 6. Comparison of classification accuracy between SVM and ProCRC classifiers across 10-fold cross-validation.

Accepted manuscript (author version)

Table 1. Classification performance using 60–40 train/test split for Bonn and HK dataset.

Dataset	Classifier	Accuracy(%)	Sensitivity (%)	Specificity (%)
Bonn	SVM	100	100	100
	ProCRC	100	100	100
HK	SVM	97.5	95	100
	ProCRC	97.5	95	100

Table 2. Classification accuracy of the proposed method across different subset combinations of the Bonn and HK dataset.

Dataset	Classification task	SVM(%)	ProCRC(%)
Bonn	A- E	100	100
	C-E	100	100
	B -E	98.75	97.5
	AB-E	99.17	98.33
	CD-E	98.33	99.17
	A-D-E	93.3	95.0
	AB-CD-E	87.5	89
	A-B	85	86.25
	A-B-C-D-E	62	64
HK	Preictal -Ictal	77.5%	80%
	Preictal-Interictal-Ictal	50%	58.33%

Table 3. Classification performance using 10-fold cross-validation.

Dataset	Classifier	Mean Accuracy (%)
Bonn	SVM	98.5
	ProCRC	99.5
HK	SVM	97
	ProCRC	96

Table 4. Performance comparison of classification methods across different assessment methods for Bonn dataset.

Method	Splitting Strategy (%)	Folding Strategy (%)
Proposed method- ProCRC	100	99.5
Proposed method- SVM	100	98.5
Ruzicka Similarity [30]	100	-
Temporal and spectral features [31]	98.15	-
LSTM [32]	97.1	-
Fusion Handcrafted and Deep learning Features [33]	-	99.82
Fractal Dimension Features and Convolutional Autoencoder Method [34]	-	99.74
Multi-domain features [35]	-	99.25
Ensemble empirical mode [36]	-	99
Spike-related features [37]	-	98.6



Accepted manuscript (author version)

Table 5. Performance comparison of classification methods across different assessment methods for Hauz Khas (HK) dataset.

Method	Splitting Strategy (%)	Folding Strategy (%)
Proposed method- ProCRC	97.5	96
Proposed method- SVM	97.5	97
neural Network Model based on Multimodal Dual-Stream Networks [38]	97.5	-
deep ensemble network with empirical wavelet transform [39]	97	-
wavelet based features and dynamic mode decomposition [40]	96.5	
Deep learning using VGG16 [41]		98.76
Signal modeling [42]	-	96.5
Spiking neural networks [43]	-	92.5

Table 6. Classification accuracy for Delta–Theta (0.5–8 Hz) vs. Beta–Gamma (12–60 Hz) on the Bonn D–E task (60–40 split).

Band Range	Classifier	Accuracy(%)	Sensitivity (%)	Specificity (%)
Beta + Gamma	SVM	100	100	100
	ProCRC	100	100	100
Delta + Theta	SVM	91.25	90	92.5
	ProCRC	92.5	87.5	97.5

